# Transcriptome analysis of Traf6 function in the innate immune response of zebrafish embryos

Stockhammer, O.W.; Rauwerda, H.; Wittink, F.R.; Breit, T.M.; Meijer, A.H.; Spaink, H.P.

Molecular Immunology 48 (2010) 179–190

Contents lists available at ScienceDirect

Molecular Immunology

journal homepage: www.elsevier.com/locate/molimm

# Transcriptome analysis of Traf6 function in the innate immune response of zebrafish embryos☆

Oliver W. Stockhammer[a], Han Rauwerda[b], Floyd R. Wittink[b], Timo M. Breit[b], Annemarie H. Meijer[a,*], Herman P. Spaink[a]

[a] Institute of Biology, Leiden University, Einsteinweg 55, 2333 CC Leiden, The Netherlands
[b] MicroArray Department & Integrative Bioinformatics Unit (MAD-IBU), Swammerdam Institute for Life Sciences, Faculty of Science, University of Amsterdam (UvA), Amsterdam, The Netherlands

ARTICLE INFO

*Article history:*
Received 7 June 2010
Received in revised form 11 August 2010
Accepted 17 August 2010
Available online 18 September 2010

*Keywords:*
Bacterial infection
Gene regulation
Signal transduction
Toll-like receptors
RNAseq
Microarray

ABSTRACT

TRAF6 is a key player at the cross-roads of development and immunity. The analysis of its *in vivo* molecular function is a great challenge since severe developmental defects and early lethality caused by *Traf6* deficiency in knock-out mice interfere with analyses of the immune response. In this study we have used a new strategy to analyze the function of Traf6 in a zebrafish-Salmonella infectious disease model. In our approach the effect of a Traf6 translation-blocking morpholino was titrated down to avoid developmental defects and the response to infection under these conditions was studied using the combination of microarray analysis and whole transcriptome deep sequencing. Transcriptome profiling of the traf6 knock-down allowed the identification of a gene set whose responsiveness during infection is highly dependent on Traf6. Expression trend analysis based on the resulting datasets identified nine clusters of genes with characteristic transcription response profiles, demonstrating Traf6 has a dynamic role as a positive and negative regulator. Among the Traf6-dependent genes was a large set of well known antimicrobial and inflammatory genes. Additionally, we identified several genes which were not previously linked to a response to microbial infection, such as the fertility hormone gene *gnrh2* and the DNA-damage regulated autophagy modulator 1 gene *dram1*. With the use of the zebrafish embryo model we have now analyzed the *in vivo* function of Traf6 in the innate immune response without interference of adaptive immunity.



## 1. Introduction

Microbial infections usually elicit a rapid and strong response of the host innate immune system. Pattern recognition receptors (PRRs), such as Toll-like receptors (TLRs) and NOD-like receptors (NLRs), enable the host to recognize pathogens by detecting conserved molecular patterns such as lipopolysaccharide (LPS), flagellin or peptidoglycan (Mogensen, 2009). Activation of these receptors will initiate the induction of pro-inflammatory cytokines and as a result a complex network of underlying signaling pathways is activated leading to a tailored inflammatory response with the ultimate goal of eradicating the pathogen. An essential protein transducing the signals emanating from various PRRs and cytokine receptors, including the TNF superfamily, TGFβ, IL-1/Toll-like and NOD-like receptors, is the TNF receptor-associated factor 6 (TRAF6) (Abbott et al., 2007; Kobayashi et al., 2004; Sorrentino et al., 2008; Yamashita et al., 2008).

Initial studies demonstrated the ability of TRAF6 to bind to CD40, RANK and IRAK-1 and showed that NF-κB signaling via TLR4 was abolished by a dominant-negative form of TRAF6 (Cao et al., 1996; Darnay et al., 1999; Galibert et al., 1998; Ishida et al., 1996; Muzio et al., 1998; Tsukamoto et al., 1999; Wong et al., 1998). Analysis of TRAF6-deficient mice revealed a critical role of TRAF6 in osteoclast development and function. Furthermore, these studies indicated an essential role of TRAF6 in IL-1 signaling, as the activation of NF-κB and JNK in response to IL-1 were absent in embryonic fibroblasts derived from TRAF6-deficient mice. Moreover, bone marrow-derived macrophages from these mutants displayed a diminished response to LPS, and dendritic cell development and function was impaired (Kobayashi et al., 2003; Lomaga et al., 1999; Naito et al., 1999).

☆ This work was financially supported by the European Commission 6th Framework Programs ZF-TOOLS (LSHG-CT-2006-037220).

* Corresponding author at: Institute of Biology, Leiden University, Einsteinweg 55, 2333 CC Leiden, The Netherlands. Tel.: +31 71 527 4927; fax: +31 71 527 4357.
*E-mail addresses:* o.w.stockhammer@biology.leidenuniv.nl (O.W. Stockhammer), j.rauwerda@uva.nl (H. Rauwerda), r.a.wittink@uva.nl (F.R. Wittink), t.m.breit@uva.nl (T.M. Breit), a.h.meijer@biology.leidenuniv.nl (A.H. Meijer), h.p.spaink@biology.leidenuniv.nl (H.P. Spaink).

0161-5890/$ – see front matter © 2010 Elsevier Ltd. All rights reserved.
doi:10.1016/j.molimm.2010.08.011

The molecular mechanism underlying signal transduction by TRAF6 upon infection is that TRAF6 exerts its function as a K63-specific RING finger E3 ligase. Upon activation of the TLR or the IL-1 receptor pathway, the association of MyD88 with the cytosolic part of the receptor results in the phosphorylation of IRAK-1 by IRAK-4. Subsequently, activated IRAK1 will bind to TRAF6 that will form a complex with the ubiquitin-conjugating enzymes Ubc13 and Uev1a resulting in the attachment of non-degradative K63-linked ubiquitin chains to TRAF6 itself and to NEMO, the regulatory component of the IKK complex upstream of NF-κB. Ubiquitination of TRAF6 will recruit the TAB2/3-TAB1-TAK1 complex resulting in the activation of TAK1. Subsequent activation of the IKK complex and MAP kinase cascades by TAK1 lead to the induction of pro-inflammatory cytokines by the NF-κB and AP-1 transcription factor complexes, respectively (Deng et al., 2000; Kanayama et al., 2004; Kawai and Akira, 2007; Wang et al., 2001). In addition to the role of TRAF6 in innate immunity, TRAF6 function was also placed in the context of adaptive immunity. Mice containing a T-cell specific deletion of TRAF6 showed the inability to maintain CD8 memory T-cells due to defective AMP-activated kinase activation and mitochondrial fatty acid oxidation after growth factor depletion (Pearce et al., 2009).

*Traf6* deficiency in mice causes severe developmental defects and early death at 17–19 days postnatal, making *in vivo* infection studies challenging. Therefore, knowledge of pathways downstream of Traf6 linking it to innate immune mechanisms has only been derived of cell culture studies. To get insights in the *in vivo* function of Traf6 in innate immunity, we have used a zebrafish embryo model system. In recent years the zebrafish (*Danio rerio*) embryo system has emerged as a model to study vertebrate innate immunity, offering several advantages that complement mammalian model systems. External development and the transparent character of the zebrafish embryo, in combination with fluorescently labeled immune cells and bacteria, allows for study of host microbe interaction and inflammation processes in the living organism (Davis et al., 2002; Hall et al., 2009; Mathias et al., 2006; Meijer et al., 2008; Redd et al., 2006; Renshaw et al., 2006; van der Sar et al., 2003; Ward et al., 2003). Analysis of the immune system of the zebrafish revealed a fully developed innate and adaptive immune system showing significant similarities to the human equivalent (Meeker and Trede, 2008; Meijer et al., 2004; Murayama et al., 2006; Stein et al., 2007; Stockhammer et al., 2009). An active innate immune system is detectable already at day one of zebrafish embryogenesis (Davis et al., 2002; Herbomel et al., 1999, 2001). By contrast, a functionally mature adaptive immune system is not active during the first three weeks of zebrafish development establishing a clear temporal separation of the innate and adaptive immune system in the zebrafish embryo. (Davidson and Zon, 2004; Lam et al., 2004; Willett et al., 1999). Therefore, the zebrafish model provides a convenient system for the *in vivo* study of the vertebrate innate immune response to infection independently from the adaptive immune response. Furthermore, morpholino based knock-down experiments facilitate the functional analysis of genes in the zebrafish embryo that otherwise lead to lethal defects in gene knock-out studies in mice. Moreover, many infection systems for zebrafish have been developed lately, allowing the analysis of gene functions under infection conditions (Lesley and Ramakrishnan, 2008; Meeker and Trede, 2008; Phelps and Neely, 2005).

In this study we aim at setting up a functional analysis system for zebrafish Traf6 in response to bacterial infection and to identify *in vivo* downstream targets of Traf6 linked to the innate immune response. Therefore we have performed transcriptome analysis of Traf6 knock-down and control embryos using the previously described *Salmonella enterica* serovar Typhimurium (hereafter referred to as *S. typhimurium*) infection model (Stockhammer et al., 2009; van der Sar et al., 2003). By titrating down the concentration of a translation-blocking morpholino we could avoid effects of Traf6 knock-down on embryo development and study the response to infection under these knock-down conditions. Multifactorial analysis of microarray data allowed the identification of a gene set whose responsiveness to *S. typhimurium* infection is highly dependent on Traf6 function. Furthermore, for the first time we have used whole transcriptome deep sequencing to analyze the response to bacterial infection with emphasis on nine differentially expressed Traf6-dependent gene clusters.

## 2. Materials and methods

### 2.1. Bacterial strains and growth conditions

*S. typhimurium* wild type (wt) strain SL1027, containing the DsRed expression vector pGMDs3, was used for the infection of zebrafish embryos (van der Sar et al., 2003). Bacteria were freshly grown overnight on LB agar plates supplemented with 100 μg/ml carbenicillin and resuspended in phosphate-buffered saline (PBS) prior to injection.

### 2.2. Zebrafish husbandry

Zebrafish were handled in compliance with the local animal welfare regulations and maintained according to standard protocols (http://ZFIN.org). Embryos were grown at 28.5–30 °C in egg water (60 μg/ml Instant Ocean sea salts). For the duration of bacterial injections embryos were kept under anaesthesia in egg water containing 0.02% buffered 3-aminobenzoic acid ethyl ester (tricaine, Sigma).

### 2.3. Morpholino knock-down experiments

For morpholino knock-down experiments, morpholino oligonucleotides (Gene Tools) were diluted to desired concentrations in 1× Danieu's buffer [58 mM NaCl, 0.7 mM KCl, 0.4 mM $MgSO_4$, 0.6 mM $Ca(NO_3)_2$, 5.0 mM HEPES; pH 7.6] containing 1% Phenol red (Sigma). To block translation of *traf6* mRNA we injected 1 nl (1 mM) per embryo of a morpholino specifically targeting the 5′ UTR region including the start codon of *traf6* (5′ GCCATATTGGCTCGGTACGGCCTC). To control for aspecific morpholino effects we used a 5 bp mismatch morpholino (1 mM, 5′ GCaATATTcGCTaGGTACaGCgTC).

### 2.4. Experimental design of the infection study

All infection experiments were performed using mixed egg clutches of ABxTL strain zebrafish. Embryos injected with the *traf6* morpholino and the 5 bp mismatch morpholino were staged at 27 h post-fertilization (hpf) by morphological criteria and approximately 250 cfu of DsRed expressing *S. typhimurium* wild type bacteria were injected into the caudal vein close to the urogenital opening as described in Stockhammer et al. (2009). As a control an equal volume of PBS was likewise injected. Pools of 20–40 infected and control embryos were collected 8 h post-infection (hpi). For the microarray analysis, the whole procedure was performed in triplicate on separate days.

### 2.5. RNA extraction

Embryos for RNA isolation were snap frozen in liquid nitrogen and subsequently stored at −80 °C. Total RNA from each sample was extracted using TRIZOL followed by a cleanup procedure with RNeasy Mini kit (Qiagen, Valencia, CA, USA), and a DNase treatment with RNase-Free DNase Set (Qiagen Valencia, CA, USA)). The

RNA concentration was measured on a nanodrop ND-100 (NanoDrop Technologies Inc., Wilmington, DE, USA) and RNA quality was checked on an Agilent 2100 BioAnalyzer (Agilent Technologies, Palo Alto, CA, USA). Total RNA samples with an RNA integrity number (RIN) > 7 were used for further analysis. These assays were performed according to the manufacturer's protocols.

### 2.6. Illumina RNA sequencing

The total RNA of the three biological samples of each treatment group, previously used for the microarray analysis, was pooled using equal amounts of RNA. To perform transcriptome sequencing, RNAseq libraries were made from 4 μg of each sample, using the Illumina mRNA-Seq Sample Preparation Kit according to the manufacturer's instructions (Illumina, Inc., San Diego). An amount of 4 pmol of each library was sequenced in one lane with a read length of 51 nt on an Illumina GAII instrument (Illumina, Inc., San Diego). The raw data were deposited in the GEO database under submission number GSE21024. Sequence reads were mapped to Ensembl transcripts (Zv8. 56) using the CLCbio Genomics Workbench version 3.6.5 (www.clcbio.com).

### 2.7. Microarray design and hybridization

A custom zebrafish genome 4 × 44 K microarray (Agilent) containing slight modifications in regard to a previous described design was used (accession no. GPL10042 in the GEO database) (Stockhammer et al., 2009). In short, a total of 600 new features based on deep sequencing results were added to the existing chip design resulting in 45,219 features, including 43,801 well-characterized genes and 1418 controls (Hegedus et al., 2009). The probes of the custom manufactured Agilent array have been reannotated by mapping all probes to the Unigene 114 (unique) sequences and the Ensembl 50 and Vega 32 transcripts using the BLAST algorithm. Technical handling of the microarrays was performed at the MicroArray Department (MAD) of the University of Amsterdam (Amsterdam, The Netherlands). In short, cyanine 3 and cyanine 5 labeled cRNA samples were prepared as described in the Amino allyl message AMP II manual (Ambion) using 0.5 μg purified total RNA as template for the reaction. Test samples were labeled with Cy3 and the common reference was labeled with Cy5. The common reference was composed by combining 1 μg of cRNA from each sample and chemical coupling of this pool with Cy5. Hybridization of 825 ng of Cy3 labeled test sample and 825 ng of Cy5 labeled common reference was performed overnight according to Agilent protocols at 65 °C. Images of the arrays were acquired using an Agilent DNA MicroArray Scanner (Agilent Technologies, Palo Alto, CA, USA).

### 2.8. Data extraction and statistical analysis

Spot intensities were quantified with Feature Extraction 9.5.1 (Agilent) as the foreground median signal intensity. Further processing of the data was performed using R (version 2.5.0), the Bioconductor MAANOVA package (version 1.6.0) (Wu et al., 2003) and Spotfire (version 7.3).

All slides were subjected to a set of quality control checks, i.e. visual inspection of the scans, examining the consistency among the replicated samples by principal components analysis, testing against criteria for signal to noise ratios, testing for consistent performance of the labeling dyes, and visual inspection of pre- and post-normalized data with box plots and RI plots.

The dataset concerned a two-factorial Latin square design, with the factors 'Morpholino treatment' (2 levels: treated and not treated) and 'Infection' (2 levels: treated and not treated). The design was completely balanced with 3 replicates each, so the experiment involved 12 observations per gene.

After log 2 transformation the data was normalized by a global LOWESS smoothing procedure. The data was analyzed using a two-stage mixed analysis of variance (ANOVA) model (Kerr et al., 2000). First, array, dye, and array-by-dye effects were modeled globally. Next, the residuals from this first model were fed into a gene-by-gene model in which we took 'Group', 'Array', and 'Dye' as factors of which 'Array' was modeled as random factor. 'Group' is defined by each unique Morpholino and Infection treatment combination. These residuals can be considered normalized expression values and used in the graphs to depict gene expression profiles. All changes were calculated from the model coefficients. For hypothesis testing a permutation based *F*s test, which allows relaxation of the assumption that the data are normally distributed, was used (2000 permutations). The significance of the differences between factor level means was tested using contrasts. To account for multiple testing, all *p*-values were adjusted to represent a false discovery rate using the method of Benjamini and Hochberg (1995). The raw data were submitted to the GEO database under accession number GSE20310.

### 2.9. Gene ontology, pathway and cluster analysis

K-means clustering was performed using Spotfire (version 7.3) Cluster initialization was set to data centroid based search and similarity measure was set to Euclidian distance. Analysis was performed on the probes retrieved by interaction term analysis with a *p*-value lower than or equal to 0.4. All identifiers lacking a valid annotation were excluded from the analysis leading to a dataset of 376 probes.

Gene ontology (GO) analysis was performed using the GeneTools eGOn v2.0 web-based gene ontology analysis software (www.genetools.microarray.ntnu.no) (Beisvag et al., 2006). Master-target analysis was performed at the level of Unigene clusters (UniGene build #105). To test for enrichment or under representation at the level of GO criteria for Biological Process (BP) we compared the UniGene identifiers retrieved from our analysis (targets) to all identifiers present on the chip (master). Identifiers tested are listed in Supplemental Tables 1 and 4 for those genes that were regulated after infection in the control and *traf6* knock-down group as well as due to *traf6* knock-down alone. All identifiers that were retrieved from the interaction term analysis are listed in Supplemental Table 6.

Pathway analysis was performed using the GenMapp software package (www.genmap.org) (Dahlquist et al., 2002). Analysis was done at the level of UniGene clusters (*D. rerio* UniGene build #114). Significance cut off was set at 1.2-fold change at $p < 0.05$. Zebrafish homologs of the genes contributing to the TLR pathway were identified by either searching the ZFIN (http://zfin.org) database or the Gene and HomoloGene database of NCBI (http://www.ncbi.nlm.nih.gov) (Supplemental Table 2).

## 3. Results

### 3.1. System for analysis of innate immune functions of Traf6

To accomplish *traf6* knock-down zebrafish embryos were injected at the one cell stage with an ATG morpholino to prevent *traf6* mRNA translation. Initial titration experiments of the *traf6* morpholino elicited a concentration-dependent effect on embryo that will be described elsewhere (Stockhammer et al., in preparation). To avoid a strong interference of developmental defects,

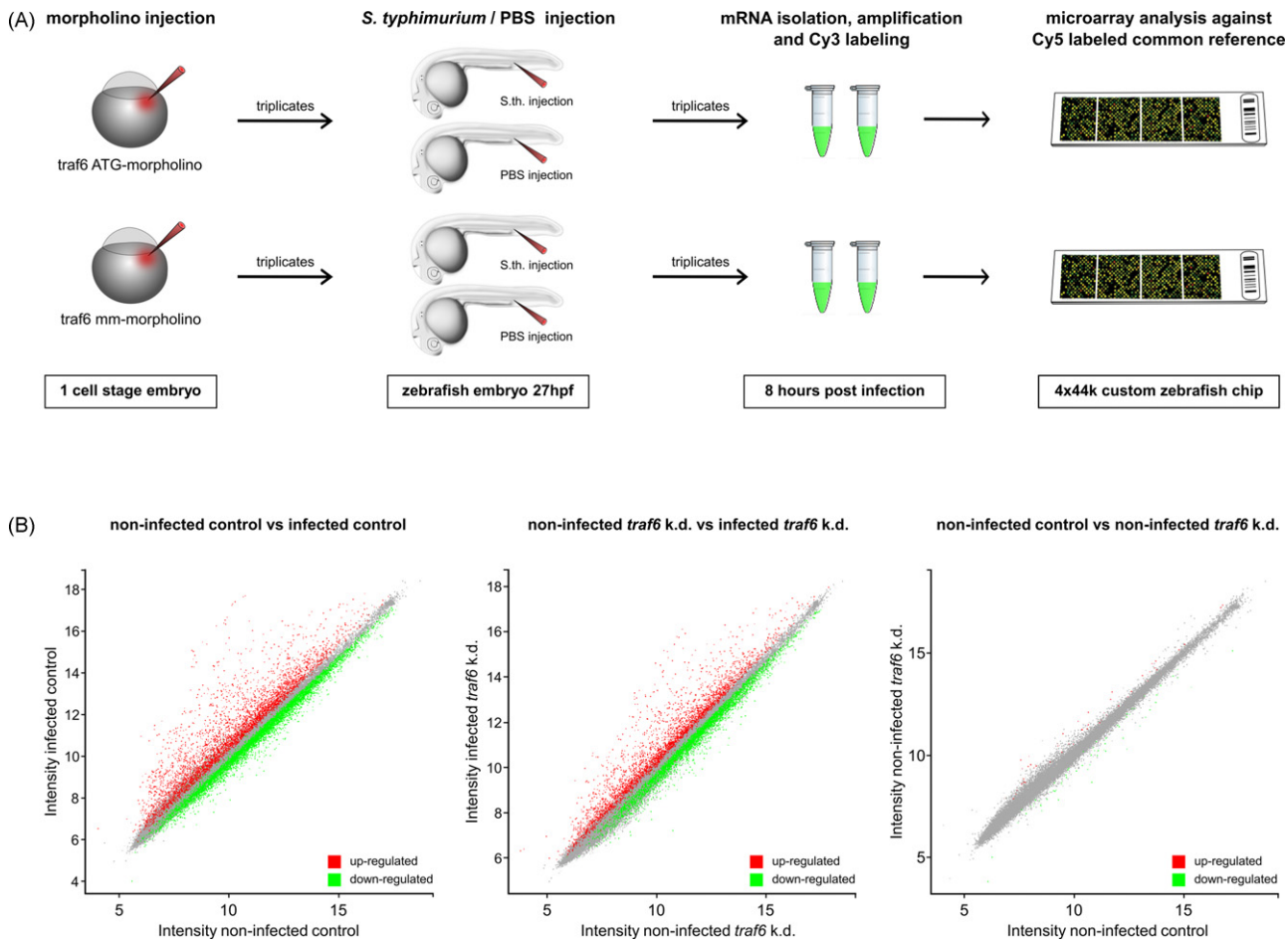


**Fig. 1.** Schematic overview of the experimental setup (A) and scatter plot illustration of the transcriptional response of the various treatment groups (B). (A) Zebrafish embryos were either injected with a *traf6* ATG morpholino or a 5 bp mismatch (mm) morpholino at the first cell stage. At 27 hpf both groups were immune challenged by injection of 250 cfu of a *S. typhimurium* strain or mock injected with PBS. The transcriptional response was subsequently analyzed at 8 h post-infection (hpi) using a common reference approach. The experiment was carried out in triplicate. (B) The scatter plots on the left side and in the middle are showing the transcriptional response upon *S. typhimurium* infection in the control (mm-morpholino) and *traf6* knock-down (k.d.) group, respectively. The scatter plot on the right shows the response provoked by *traf6* knock-down independently of the infection.

all infection assays were performed using a concentration of 1 mM *traf6* morpholino that did not elicit developmental effects. To be able to discriminate between the specific effect of the *traf6* knock-down and possible aspecific morpholino effects in our assay a control group was treated with a 5 bp mismatch *traf6* morpholino. At 27 hpf both groups were either immune challenged by injection of 250 cfu of a *S. typhimurium* wild type strain or mock injected with PBS. The transcriptional response was subsequently analyzed at 8 h post-infection (hpi) (Fig. 1A). Initial analysis of the datasets demonstrated a robust response to the infection in the control as well as in the *traf6* knock-down group. At the UniGene cluster level a total of 3720 genes ($p < 0.05$ and a fold change $\leq -1.2$ and $\geq 1.2$) were regulated upon bacterial challenge in the control group. In contrast, a reduced response showing a total of 2840 differentially regulated genes ($p < 0.05$ and a fold change $\leq -1.2$ and $\geq 1.2$) was noticeable in the *traf6* knock-down group (Fig. 1B, Supplemental Table 1). The *S. typhimurium*-induced expression signatures of both the control and the *traf6* knock-down groups were consistent with the published results of Stockhammer et al. (2009) and include all genes previously validated by Q-PCR in that study. As shown by projection of the microarray data on a GenMapp of the TLR-signaling pathway, the *S. typhimurium*-induced gene sets of both groups included several TLR pathway components and downstream targets (Fig. 2, Supplemental Table 2). Furthermore, GO-analysis on the zebrafish gene identifiers by master-target testing on the level of Biological Process revealed among others the GO-terms immune system process and response to stimulus as significantly ($p < 0.05$) enriched in both groups (Supplemental Table 3). Interestingly, genes that were clustered under the GO-term reproduction were also significantly enriched in the up-regulated fraction. In contrast, only minor differences were provoked by *traf6* knock-down itself, indicating that our titration of the morpholino to avoid the developmental effect has been effective. In total 20 genes were up- and 35 genes were down-regulated by traf6 knock-down in the absence of infection ($p < 0.05$, fold change $\leq -1.2$ and $\geq 1.2$) (Fig. 1B, Supplemental Table 4). Among the group of up-regulated genes we identified genes such as *stc1* (*stanniocalcin 1*, fc = 2.62), a gene involved in $Ca^{2+}$ uptake in zebrafish, as well as *zgc:77734* (fc = 2.57), showing similarities to the human DBI (diazepam binding inhibitor) gene. Examples of genes down-regulated by traf6 knock-down in the absence of infection are *or111-3* (fc = −3.8), a member of the fish odorant receptor family, and *he1a* (*hatching enzyme 1a*, fc = −2.68) as well as *rcv1* (*recoverin*, fc = −2.15) and *anterior gradient homolog 2* (*agr2*, fc = −1.89) (supplemental Table 4).

### 3.2. Statistical analysis of the effect of traf6 knock-down on the infection response

In order to find those genes that were specifically differentially regulated in the *traf6* knock-down group in comparison to the

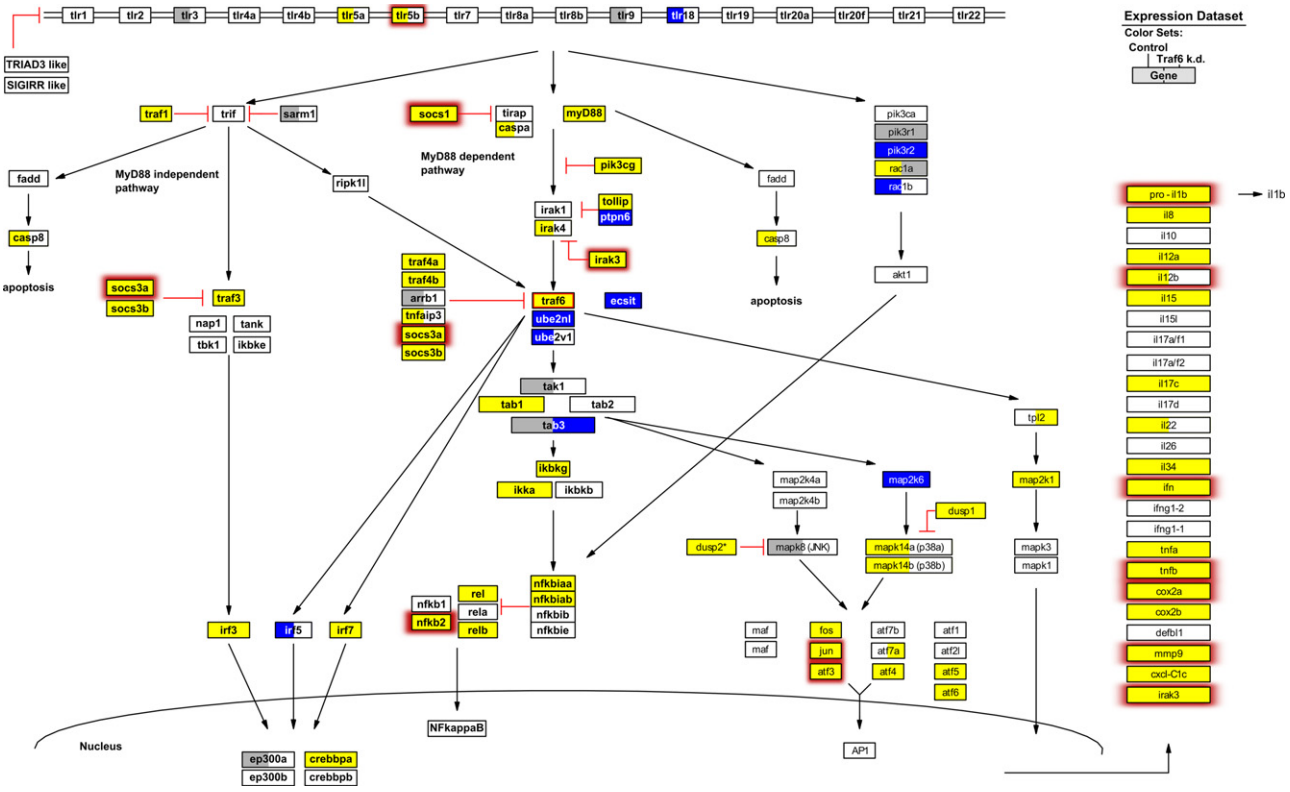


**Fig. 2.** GenMapp analysis of the immune response to *S. typhimurium* infection in the TLR pathway in control and *traf6* knock-down embryos. Expression profiles of the control and *traf6* knock-down groups at the 8 hpi time point (infected versus non-infected, FDR-corrected $p$-value < 0.05 and fold changes $\geq$1.2 and $\leq$−1.2) were simultaneously mapped on the TLR pathway. Gene boxes are colour coded with the control-morpholino treatment (Control) on the left and *traf6* knock-down (Traf6 k.d.) on the right side. Up-regulation is indicated in yellow, down-regulation in blue. The position of *traf6* in the pathway is highlighted by a red border of the gene box. Genes that failed the fold change cut off are depicted in gray and genes that were not significantly regulated are represented in white. Highlighting of gene boxes by red shading indicates that the *S. typhimurium*-induced gene expression level was lower in *traf6* knock-down embryos than in control embryos, based on microarray expression trend analysis as well as RNAseq analysis. The pathway is based on knowledge of TLR signaling in mammalian species and it should be noted that most interactions remain to be experimentally confirmed in zebrafish. (For interpretation of the references to colour in this figure legend, the reader is referred to the web version of the article.)

control group upon infection, the interaction term was analyzed. Interaction is defined as the dependence of the effect of one factor (here gene knock-down by morpholino treatment) on the level of another factor (here immune challenge by infection). In terms of the analysis of variance (ANOVA) model, the interaction term measures the deviation from an expected value based on the additive combinations of the morpholino and infection means. A large positive deviation of this sort is called synergism, in which case the simultaneous morpholino and infection treatment gives rise to an expression level that deviates from the additive combination of the morpholino and infection treatment alone. A negative deviation, i.e. when the combined infection and morpholino application gives rise to a smaller effect than one could expect from the additive combination of the two effects separately, can be called interference. Synergy can be in the direction of overexpression or underexpression. In the former, a gene has a higher expression in the combined treatment than one could expect on the basis of the additive combination of the separate treatments. In the latter, a gene has an even lower expression in the combined treatment than one could expect on the basis of the additive combination of the separate treatments.

To specifically identify genes that were most highly dependent on Traf6 for their transcriptional response to a bacterial infection we examined all genes that were significant in the interaction term analysis with a stringent FDR-corrected $p$-value smaller than 0.15 (Table 1). The expression profiles of 28 identified genes corresponding to this criterion are shown in a heatmap (Fig. 3). For the majority of these genes (20 out of 28) the *S. typhimurium*-induced gene expression levels were much lower in the *traf6* knock-down group than in the control group (Fig. 3), indicating that the infection-mediated induction of these genes is dependent on *traf6*. Among these were several with a well established immune function like *hamp2*, *mmp9*, *mmp13*, *tnfb*, *il1b*, *ncf1*, *crfb4* and *zgc:103580*, the zebrafish ortholog of the human acute phase response gene serum amyloid protein A. In addition to two members of the matrix metalloproteinase family (*mmp9* and *mmp13*), the group of 20 genes with a reduced infection response in *traf6* knock-down embryos also included the metalloproteinase inhibitor gene *timp2b* (*tissue inhibitor of metalloproteinase 2b*). This group also included *zgc:112143*, a gene homologous to the human *STEAP4* gene (also known as *TNFAIP9*, tumor necrosis factor alpha-induced protein 9), that we previously found to be induced with alternative splice forms during *Mycobacterium marinum* infection in adult zebrafish (Hegedus et al., 2009). On the other hand, the gene group showing a reduced infection response in *traf6* knock-down embryos also included genes that were previously not linked to immune function or TRAF6 signaling like *plekhf1* (*pleckstrin homology domain containing, family F*), *clic2* (*chloride intracellular channel 2*), *pfkfb3* (*6-phosphofructo-2-kinase/fructose-2,6-biphosphatase 3*), *gnrh2* (*gonadotropin-releasing hormone 2*), and *dram1* (DNA-damage regulated autophagy modulator 1).

In addition to the 20 genes showing a reduced infection-mediated induction in *traf6* knock-down embryos, the statistical analysis also identified 4 genes (*cxcl12b*, *atp1a1a.3*, *zgc:55418* and *zgc:85900*) that appeared to be dependent on Traf6 for their negative regulation during infection. These genes were down-regulated by infection in control embryos but not or

**Table 1**
Genes dependent on Traf6 during Salmonella infection.

| Gene symbol | Description | *p*-Value | UniGene ID | ENS50 ID | K-means cluster | RNAseq |
|---|---|---|---|---|---|---|
| gnrh2 | Gonadotropin-releasing hormone 2 | 0.06 | Dr.84757 | ENSDARG00000044754 | 8 | + |
| clic2 | Chloride intracellular channel 2 | 0.06 | Dr.84618 | ENSDARG00000010625 | 8 | + |
| hamp2 | Hepcidin anti-microbial peptide 2 | 0.08 | Dr.89447 | ENSDARG00000053227 | 8 | + |
| zgc:56292 | Similar to thyroid hormone receptor interactor 10 | 0.09 | Dr.79814 | ENSDARG00000028524 | 1 | n.d. |
| pfkfb3 | 6-Phosphofructo-2-kinase/fructose-2,6-biphosphatase 3 | 0.09 | Dr.78868 | ENSDARG00000001953 | 8 | + |
| timp2b | Tissue inhibitor of metalloproteinase 2b | 0.09 | Dr.81512 | ENSDARG00000075261 | 8 | + |
| dram1 | DNA-damage regulated autophagy modulator 1 | 0.09 | Dr.77501 | ENSDARG00000045561 | 7 | + |
| zgc:112143 | STEAP family member 4 homolog | 0.09 | Dr.76505 | ENSDARG00000055901 | 7 | + |
| crfb4 | Cytokine receptor family member b4 | 0.11 | Dr.14717 | ENSDARG00000068711 | 7 | + |
| wu:fk20h09 | Similar to pyruvate dehydrogenase complex, component X | 0.11 | Dr.140666 | | 7 | n.a. |
| zgc:103580 | Serum amyloid A1 homolog | 0.11 | Dr.13131 | ENSDARG00000045999 | 7 | + |
| cxcl12b | Chemokine (C-X-C motif) ligand 12b | 0.11 | Dr.27045 | ENSDARG00000055100 | 9 | + |
| il1b | Interleukin 1, beta | 0.11 | Dr.30443 | ENSDARG00000005419 | 7 | + |
| sc5d | Sterol-C5-desaturase | 0.11 | Dr.119848 | ENSDARG00000044642 | 4 | – |
| mmp13 | Matrix metalloproteinase 13 | 0.12 | Dr.81475 | ENSDARG00000012395 | 7 | + |
| mmp9 | Matrix metalloproteinase 9 | 0.12 | Dr.76275 | ENSDARG00000042816 | 8 | + |
| tnfb | Tumor necrosis factor b | 0.12 | Dr.94015 | ENSDARG00000013598 | 8 | + |
| wu:fk35f04 | Hypothetical protein containing S-100 domain | 0.12 | Dr.148687 | | 7 | n.a. |
| stc1 | Stanniocalcin 1 | 0.12 | Dr.88421 | ENSDARG00000058476 | 2 | + |
| atp1a1a.3 | ATPase, $Na^+/K^+$ transporting, alpha 1a.3 polypeptide | 0.12 | Dr.10713 | ENSDARG00000039131 | 9 | + |
| npsn | Nephrosin | 0.12 | Dr.79156 | ENSDARG00000010423 | 2 | – |
| wu:fd60d02 | Transcribed locus | 0.12 | Dr.79931 | | 8 | n.a. |
| wu:fe16d09 | Transcribed locus | 0.12 | Dr.80006 | | 7 | n.a. |
| zgc:55418 | Similar to ABI gene family, member 3 (NESH) binding protein | 0.12 | Dr.14064 | ENSDARG00000071095 | 9 | + |
| zgc:85900 | Olfactomedin 2 like | 0.14 | Dr.85843 | ENSDARG00000007015 | 9 | + |
| ncf1 | Neutrophil cytosolic factor 1 | 0.14 | Dr.2973 | ENSDARG00000033735 | 8 | + |
| plekhf1 | Pleckstrin homology domain containing, family F | 0.14 | Dr.80998 | ENSDARG00000027852 | 8 | + |
| si:dkey-7c18.24 | Hypothetical protein | 0.14 | Dr.104301 | ENSDARG00000041433 | 7 | + |

Listed genes were identified by interaction term analysis. Significance cut off values were set to $p < 0.15$ (FDR). All genes indicated as + were confirmed by RNAseq analysis, whereas genes indicated as – were not. Four genes indicated as not applicable (n.a.) lacked an ensdart identifier and could therefore not be verified by RNAseq analysis. For one gene indicated as not detectable (n.d.) not enough RNA sequence reads were obtained (<1 mapped reads per million total reads). K-means cluster identifiers refer to Fig. 5.

to a lower extent in *traf6* knock-down embryos (Fig. 3, Table 1). Four other genes showed a more complex dependency on Traf6, with opposite regulation in knock-down embryos and controls (*sc5d*) or with expression levels affected both in the absence and presence of infection (*zgc:56292*, *stc1*, *npsn*).

In conclusion, based on the interaction term analysis we identified genes that are dependent on Traf6 activity for their positive or negative regulation during *S. typhimurium* infection of zebrafish embryos.

### 3.3. Confirmation of Traf6-dependent genes by RNA deep sequencing

In order to confirm the microarray data we subjected the pooled RNA samples of the three biological replicates of each treatment group to Illumina RNA sequencing (RNAseq). Approximately 15 million reads were obtained for each of the four RNAseq libraries (control, control infected, *traf6* knock-down, *traf6* knock-down infected) and approximately 10 million reads per library could be mapped to the Ensembl transcript database based on the Zv8 genome sequence. Next we compared the sequence read counts (mapped reads per million total reads) between the treatment groups (Supplemental Table 6). For 21 of the 28 genes that were significant in the interaction term analysis, we found that the RNAseq data confirmed the microarray results. This included 16 of the 20 genes positively dependent on Traf6 during infection and all 4 of the genes negatively dependent on Traf6 during infection. Representative examples of these positively (*il1b*, *mmp9*, *mmp13*, *timp2b*) and negatively (*atp1a1a.3*) regulated genes are shown in Fig. 4. In five cases the microarray data could not be validated by RNAseq because transcripts for these genes were not present in the Ensembl database or not enough RNAseq reads were obtained (<1 mapped reads per million total reads). In only two cases, the RNAseq data did not confirm the microarray data. Both these cases (*sc5d*, *npsn*) were genes showing a complex dependency on Traf6 as described above. In conclusion, RNAseq analysis validated the interaction term analysis for most of the genes whose induction or repression during *S. typhimurium* infection was found to be dependent on Traf6.

### 3.4. Expression trend analysis

Since the knock-down conditions of Traf6 can be considered to be incomplete, we also wanted a broader overview of the effects of *traf6* knock-down in an expression trend analysis of the microarray data using a less stringent criterion: a FDR-corrected *p*-value of smaller than 0.4 retrieved from the interaction term. First, we analyzed these probes by enrichment analysis based on gene

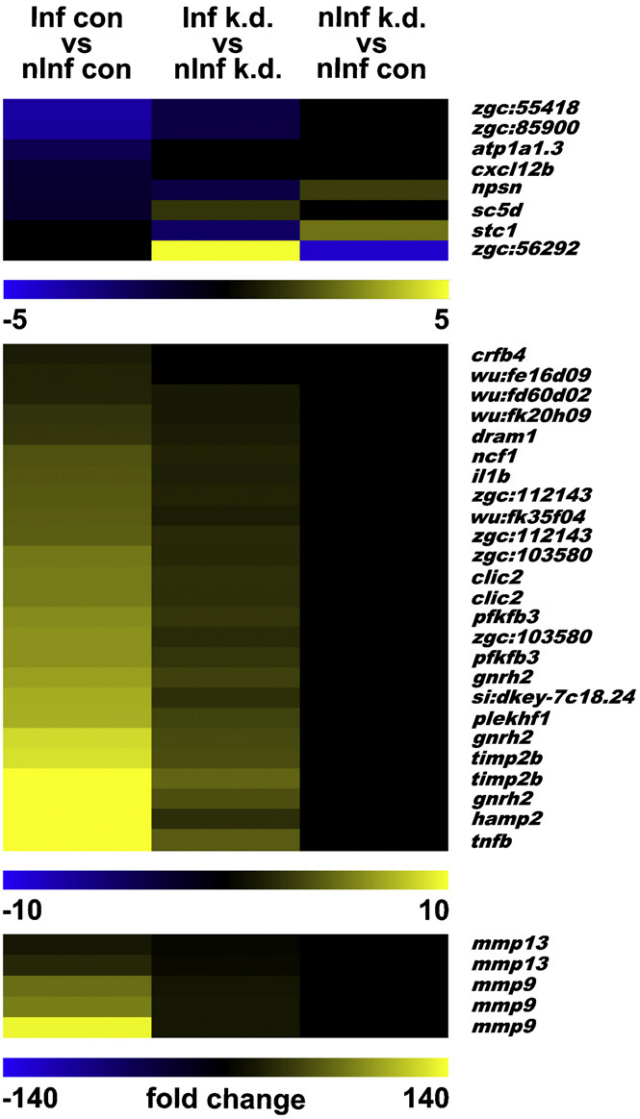


**Fig. 3.** Heatmap showing the expression profiles of genes dependent of Traf6 during *S. typhimurium* infection as identified by interaction term analysis. Up-regulated expression is indicated in yellow, down-regulated expression in blue, and non-significantly changed expression in black. The level of up- or down-regulated expression is depicted by increasing brightness of yellow and blue colour, on three different scales for genes in different expression ranges. Note that several genes are represented by multiple probes on the microarray that showed significantly changed expression in the interaction term analysis. Gene descriptions and database identifiers are shown in Table 1. Column labels: infected control-morpholino treated group (Inf con), non-infected control-morpholino treated group (nInf con), infected *traf6* knock-down group (Inf k.d.), non-infected *traf6* knock-down group (nInf k.d.). (For interpretation of the references to colour in this figure legend, the reader is referred to the web version of the article.)

ontology (GO) annotation. A significant enrichment was demonstrated for genes clustering under the biological process GO-terms immune system process ($p < 0.05$), response to stimulus ($p < 0.05$), and multi-organism process ($p < 0.05$), demonstrating a clear effect of *traf6* knock-down on the immune response to *S. typhimurium* (Supplemental Table 5).

Following up the GO-term analysis, we subjected the selected probes to K-means cluster analysis, allowing for the visual discrimination between synergism and interference of the interaction term. Probes missing a valid annotation were excluded from the analysis. The remaining 376 probes, representing 233 genes, were categorized into 9 clusters (Fig. 5, Supplemental Table 6). The microarray expression trends of 246 of these probes, representing 146 genes, were confirmed by the RNAseq data (Supplemental Table 6, with representative examples in Fig. 4), indicating the validity of these results despite the use of a less stringent criterion in the interaction term analysis.

Genes indicated by clusters 1 and 2 were, respectively, up- or down-regulated upon infection under the *traf6* knock-down condition, whereas only minor and in the majority not significant changes were observed in the control group. These two clusters contain such genes as *zgc:1154057* (*transcriptional adaptor 2-like*) in cluster 1, and *cpox* (*coproporphyrinogen oxidase*) and *stc1* (*stanniocalcin 1*) in cluster 2 (Supplemental Table 6, Fig. 4). Clusters 3 and 4 show an opposing trend in gene regulation upon infection between the control and *traf6* knock-down groups. Cluster 3 was not considered further, since regulation of the few genes in this cluster were not confirmed by the RNAseq data. Genes in cluster 4 were consistently up-regulated in the *traf6* knock-down group upon infection, while down-regulated or non-responsive in the control group, with examples such as *zgc:92061* (similar to keratin 17) and *tm7sf2* (transmembrane 7 superfamily member 2) (Supplemental Table 6, Fig. 4). A common trend in gene regulation is observed in clusters 5 to 8, where infection leads to a consistent up-regulation in the control groups and weaker up-regulation (clusters 7 and 8) or unchanged expression (clusters 5 and 6) in the *traf6* knock-down groups. Finally, cluster 9 consists of those genes that were strongly down-regulated by infection in the controls, while showing a weaker or no down-regulation in *traf6* knock-down embryos.

For further analysis we concentrated on the genes that were dependent on Traf6 for their induction (clusters 5–8) or repression (cluster 9) during *S. typhimurium* infection. From the total of 124 genes with Traf6-dependent induction and 32 genes with Traf6-dependent repression, the microarray expression trend of 105 and 22 genes, respectively, could be confirmed by the RNAseq data (Supplemental Table 6, with representative examples in Fig. 4). We categorized these Traf6-dependent genes into functional groups based on gene ontology terms and using references to gene function of their mammalian homologs in the NCBI Entrez Gene database (Fig. 6). A notable fraction of the Traf6-dependent infection-induced genes play a well established role in the immune response, for example as cytokines or interferons (e.g. *il1b*, *tnfb*, *CCL-C5a*, *ifnphi1*), in complement activation or the acute phase response (e.g. *cfb*, *zgc:103580*), in prostaglandin biosynthesis (*pgts2a*), or in microbial killing (e.g. *ncf1*, *hamp2*). Many of the Traf6-dependent infection-induced genes are involved in signal transduction and transcriptional activation or repression. This includes the *tlr5b* gene, important for the response to flagellin, negative regulators of TLR-signaling (*irak3*, *socs3a*) as well as transcription factors (*atf3*, *jun*, *nfkb2*) activated by the TLR pathway (Figs. 2 and 6). Other examples of Traf6-dependent signal transduction genes include *fas* (*TNF receptor superfamily*, *member 6*), *tgfb1* (*transforming growth factor*, *beta 1*), *ctnnb2* (beta-catenin2), *wnt10*a, and small gtpase genes (*rhogb*, *rhoab*). In addition to the above-mentioned Traf6-dependent members of the matrix metalloproteinase family (*mmp9* and *mmp13*) and metalloproteinase inhibitor gene (*timp2b*), the induction of several other genes involved in proteolysis was Traf6-dependent (e.g. *adam8a*, *agt*, *psme1|2*, *serpine1*). Finally, Traf6-dependent infection-induced gene groups were linked to apoptosis (e.g. *bcl2l*, *dram1*), cell adhesion (e.g. *cldnc*), transporter activity (e.g. *clic2*, *slc13a2*), or encoded enzymes involved in metabolic processes (e.g. *acsl4l*, *pfkfb3*, *dgat1b*) (Fig. 6).

Not only the infection-induced gene groups, but also the gene groups that were dependent on Traf6 for their repression during infection included genes for cytokines (*cxcl12b*, *cxcl14*), transporters (*atp1a1a.3*, *slc56a11*), enzymes (*ca4a*, *sulf2*) and signal transduction proteins (e.g. *efnb3*, *nbl1*). In addition, several other

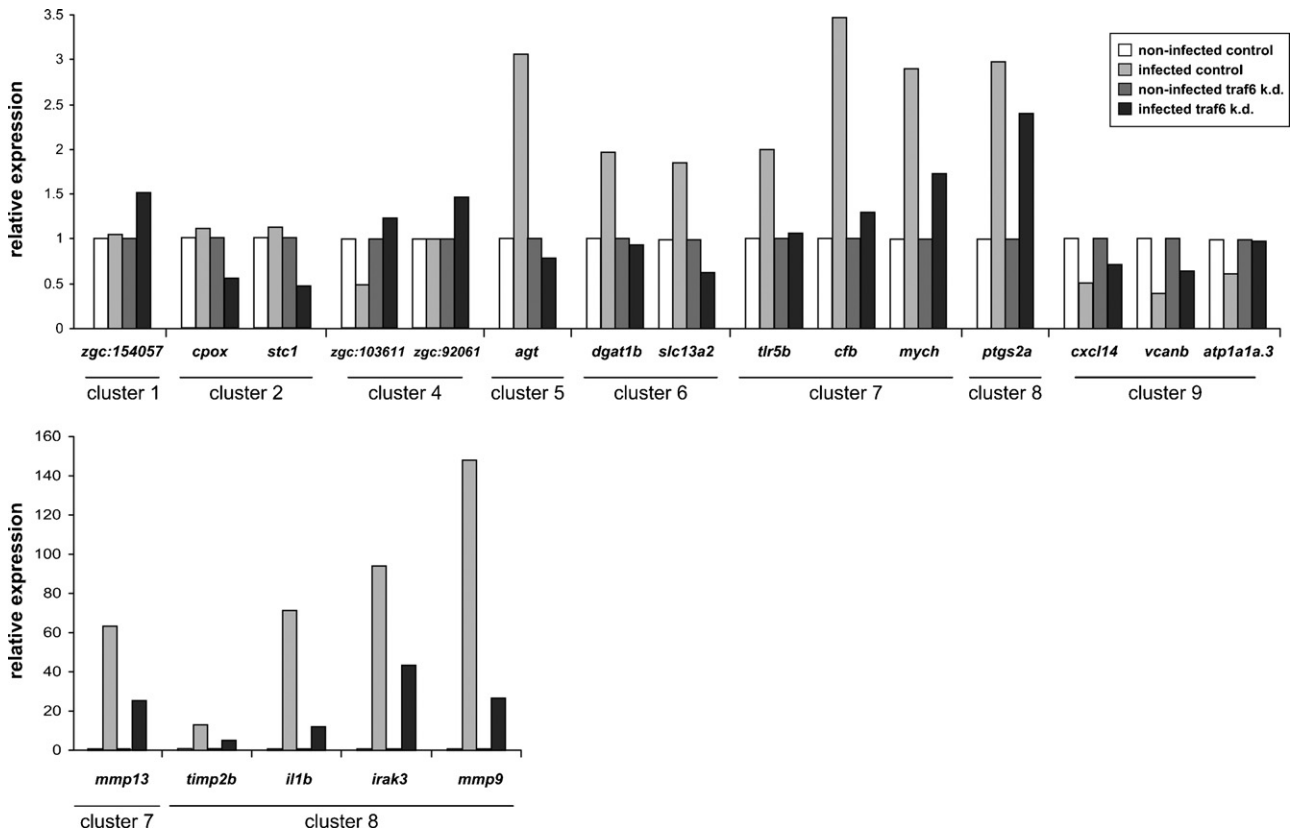


**Fig. 4.** RNAseq validation of microarray results. RNAseq data are shown for representative examples of genes for which the microarray expression trend was confirmed by RNAseq read counts of the four treatment groups (non-infected control, infected control, non-infected *traf6* knock-down, infected *traf6* knock-down). Bars indicate the relative expression of the different treatment groups based on the number of mapped sequence reads per million of total reads. For every gene the value of the uninfected control group is set to 1 and the expression level of the gene in the treatment group is calculated relative to the control value. Two different scales are used for genes in different ranges of induction level upon *S. typhimurium* infection. Cluster numbers refer to the K-means clustering in Fig. 5. The complete overview of genes for which the microarray expression trend was confirmed by RNAseq is given in Supplemental Table 6.

genes, for example *vcanb*, encoding a member of the hyaluronan (HA)-binding proteoglycans, were repressed by infection in a Traf6-dependent manner (Fig. 6).

Taken together, based on the expression trend analysis of the microarray data and validation by RNAseq, we conclude that Traf6 has a dynamic role as a positive and negative regulator of genes responsive to *S. typhimurium* infection in zebrafish embryos, including a large set of well known anti-microbial and inflammatory genes as well as genes not previously linked to the immune response or to Traf6 function.

## 4. Discussion

The fact that TRAF6 is a key player at the cross-roads of development and immunity makes the analysis of its *in vivo* molecular function a great challenge (Lomaga et al., 1999; Naito et al., 1999; Xiao et al., 2003). Severe developmental defects and early lethality caused by *Traf6* deficiency in knock-out mice interfere with analyses of the immune response. In study we have developed a new approach to analyze the function of Traf6 in a zebrafish acute infectious disease model.

In a separate study we have shown that at high concentrations of Traf6 morpholino developmental aberrations were clearly visible at early gastrulation stage, even prohibiting further development at concentrations above 1 mM. This effect was shown to be specific by comparisons of two morpholinos directed at Traf6 and control morpholinos, including a mismatch morpholino (Stockhammer et al., in preparation). Such an effect was not observed with morpholinos directed at other genes of the TLR pathway such as MyD88 (Van der Sar et al., 2006). To study the function of Traf6 during infection at later stages of development one of the used Traf6 morpholinos was titrated in such a way that developmental defects were brought back to an identifiable non-dominant factor in the transcriptome analyses at 35 h post-fertilization. The results show that under these knock-down conditions, it was possible to identify a large gene set (Table 1) whose responsiveness during *S. typhimurium* infection is highly dependent on Traf6.

We have previously reported on the transcriptome response after Salmonella infection using microarray studies and identified several MyD88-dependent genes using quantitative RT-PCR. In zebrafish embryos Salmonella infection causes a lethal infection within 24 h. This makes the Salmonella infection model not very suitable for performing direct measurements of the proliferation of the infectious agent, but it has been shown to be very useful to measure transcriptome responses within several hours after infection. A large set of inflammatory genes, including homologs of many human immune-related transcription factors and other innate immune signaling components, is induced in this infection system (Stockhammer et al., 2009). The results presented here confirm the previous data but we now have added for the first time complete transcriptome deep sequencing technology to further validate the Salmonella infection-dependent datasets. Furthermore, we have now coupled transcriptome analysis to functional studies by identifying the Traf6-dependent subset of genes. Among the genes that are highly dependent on Traf6 for their induction in response to *S. typhimurium* infection a subset of well known immune system-associated genes such as *il1b*, *mmp9*, *mmp13*, *hamp2*, and *tnfb* was

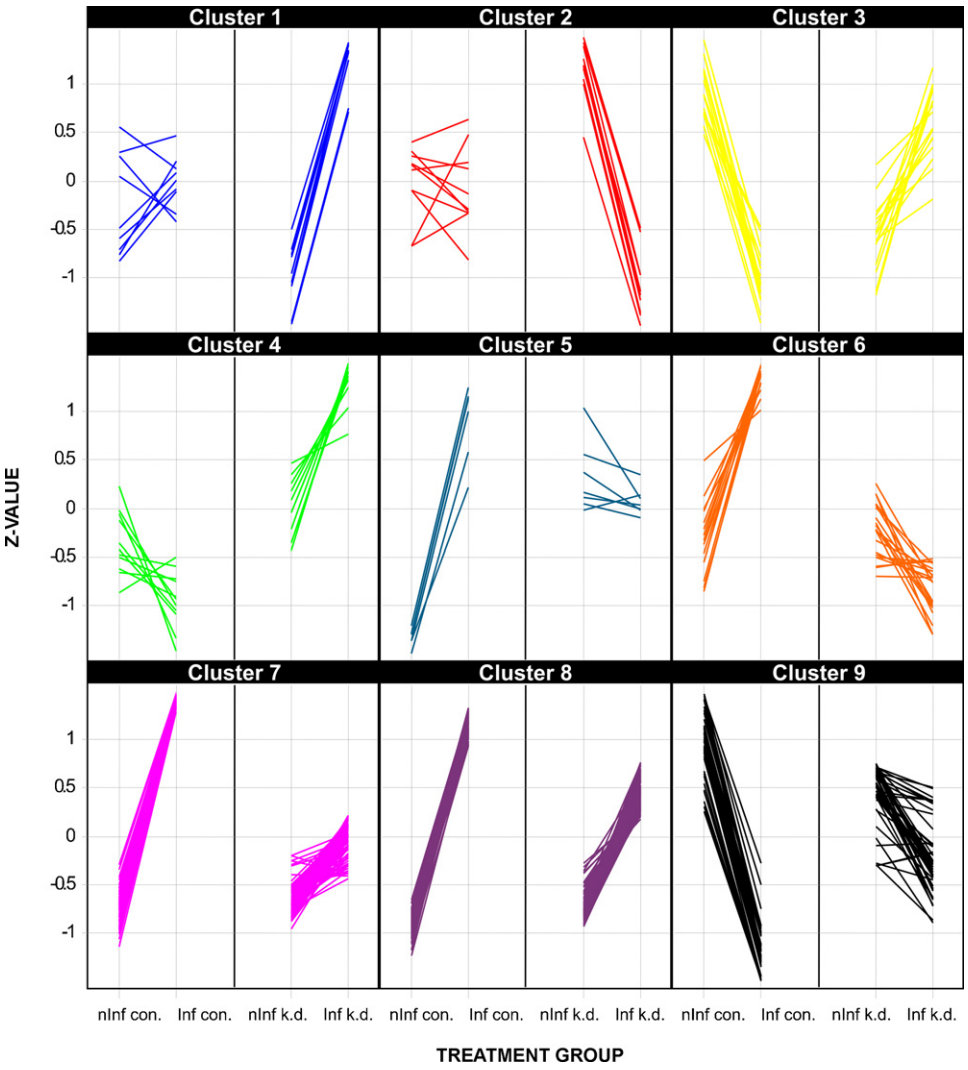


**Fig. 5.** Trend analysis of the interaction term by K-means clustering. For a broader analysis of the effects of *traf6* knock-down all retrieved probes with an FDR-corrected *p*-value lower than 0.4 were clustered using the K-means cluster function in SPOTFIRE. All probes lacking a valid annotation were excluded from the analysis resulting in a final set of 376 probes. The identified trend in the control group is illustrated on the left side of each cluster expressed by the *z*-score of each probe between the non-infected (nInf con) and the infected (Inf con) control-morpholino treated group. On the right side the corresponding trend of the non-infected (nInf kd) versus the infected (Inf kd) group under the *traf6* knock-down condition is illustrated. All probes that contribute to the distinct clusters are listed in Supplemental Table 6.

found, demonstrating a specific *in vivo* effect of Traf6 on the innate immune response. Previously we could show that *il1b* and *mmp9* are downstream targets of the zebrafish TLR pathway. The dependency of the expression of these genes on Traf6 is consistent with this study and supports the specificity of the morpholino knock-down (Stockhammer et al., 2009). It was shown in mouse that MMP-9 can also be activated upon RANKL stimulation via TRAF6, p38 and ERK1/2 (Sundaram et al., 2007). RANKL is a member of the tumor necrosis factor (ligand) superfamily and is an important activator of osteoclasts, cells involved in bone resorption. Although osteoclasts only develop in zebrafish larvae after several weeks it is not unlikely that these pathways are conserved during embryonic development (Witten et al., 2001). Several of the other Traf6-dependent genes that are linked to the TLR/IL1R-pathway are also corroborated in other model systems. It was shown that the regulation of hepcidin (HAMP1) is facilitated via the TLR pathway in mice-derived macrophages upon bacterial infection (Koening et al., 2009). Another example shown in human chondrocytes is that activation of MMP-13 through the IL1-signaling pathway was strongly impaired after *traf6* knock-down (Ahmad et al., 2007). Interestingly, also the induction of a tissue inhibitor of metalloproteinase function, Timp2b was dependent of Traf6 during zebrafish embryo infection. The expression of *timp2b* was also found to be induced during mycobacterium infection in zebrafish embryos, which was suggested to function as a compensatory response to increased *mmp9* activity (Volkman et al., 2010). Furthermore, human TIMP2 has been linked to cancer progression and has been found to be a marker for dendritic cell response to HIV infection (Solis et al., 2006). The known immune response genes that we showed to be induced in a Traf6-dependent manner also included components of the TLR-signaling pathway, such as *tlr5b* and *irak3*. It remains a question whether the regulation of the above-mentioned genes is mediated via the TLR pathway itself or via another Traf6-directed pathway. For instance Salmonella infection also regulated *tgfb1* in the TGF-beta pathway in a Traf6-dependent manner. Therefore, the poorly understood interrelatedness of the TGF-beta and TLR-signaling pathways remains an important subject for future investigations.

Other Traf6-dependent infection-induced genes, such as *dram1* (*DNA-damage regulated autophagy modulator 1*) and *gnrh2*

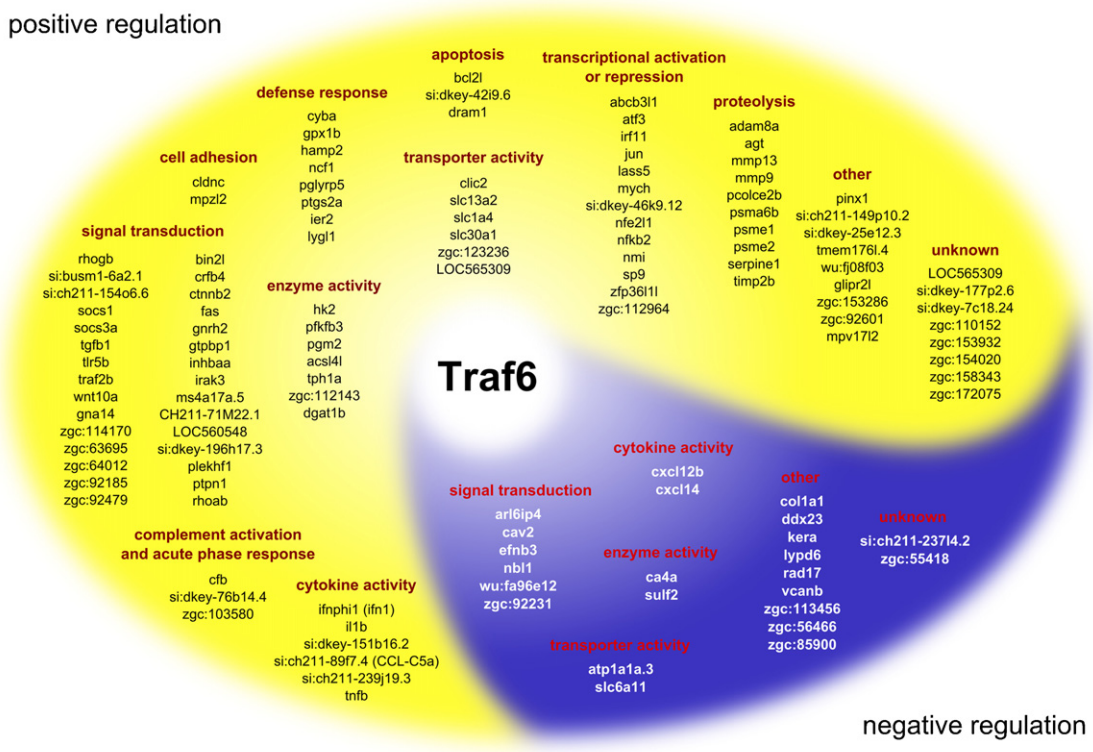


**Fig. 6.** Schematic overview of the Traf6-dependent gene groups during *S. typhimurium* infection. Genes that are dependent on Traf6 for their induction during infection (positive regulation) are in the yellow area of the scheme and genes that depend on Traf6 (negative regulation) for their repression during infection are in the blue area. Genes positively regulated by Traf6 belong to clusters 5–8 in the microarray expression trend analysis in Fig. 5, and genes negatively regulated by Traf6 belong to cluster 9. The microarray expression trend of all genes in the scheme was in agreement with RNAseq data. (For interpretation of the references to colour in this figure legend, the reader is referred to the web version of the article.)

(*gonadotropin-releasing hormone 2*), have until know not been directly associated with TRAF6 function. Human homologs of *dram1* are activated by p53 as a requirement to induce autophagy and damage-induced programmed cell death (Crighton et al., 2006; O'Prey et al., 2009). As recently highlighted in several studies, the autophagy pathway is also important for the control of intracellular pathogens and therefore the link with Traf6 function is relevant for Salmonella infection (Kumar et al., 2010; Munz, 2009). In the zebrafish embryo *gnrh2* has been linked to central nervous system development (Wu et al., 2006). However, next to the well established function of GnRH in mammalian reproduction, an immune regulatory function was suggested as well (Chen et al., 1999; Tanriverdi et al., 2003). In fact, Tanriverdi et al. (2003) have discussed that immune and reproductive function are intrinsically linked in a so-called hypothalamic–pituitary–gonadal axis (60). Recently it was shown that GnRH treatment of mice macrophages *in vitro* leads to elevated $Ca^{2+}$ uptake and an impaired generation of NO and suppression of iNOS after LPS/INF-γ treatment (Min et al., 2009). A function of Traf6 in $Ca^{2+}$ homeostasis is suggested by the fact that there is an interference effect of *traf6* knock-down and *S. typhimurium* infection on *stanniocalcin* (*stc1*) regulation. The mammalian homolog of *stanniocalcin* is involved in inhibition of transendothelial migration of human macrophages and T-lymphocytes (Chakraborty et al., 2007). In addition *stanniocalcin* was also shown to stimulate osteoblast differentiation in rat calvaria cells (Yoshiko et al., 2003). In a broader sense, Traf6 is probably involved in other ion transport processes. For instance the induction of *chloride intracellular channel 2* (*clic2*) by Salmonella infection is highly dependent of Traf6 function. Furthermore, the negative regulation of *ATPase, $Na^+/K^+$ transporting, alpha 1a.3 polypeptide* (*atp1a1a.3*) during *S. typhimurium* infection is blocked by *traf6* knock-down.

In addition to the annotated genes we also have identified Traf6 targets of which no annotation could be derived either for zebrafish, mouse or human orthologs (Supplemental Table 6, Fig. 6). Even domain searches could not identify a possible function. Since the expression levels of some of these genes are both strongly affected by Salmonella induction at early time points (Stockhammer et al., 2009) and are strongly dependent on Traf6 function, the further study of the function of these genes in the vertebrate immune system is of great interest.

Interestingly, we find the induction of several metabolic genes to be dependent on Traf6 function during Salmonella infection in 1-day old embryos, suggesting a possible role in the immune response. For example, expression of *6-phosphofructo-2-kinase* (*pfkfb3*), *hexokinase 2* (*hk2*), and *diacylglycerol O-acyltransferase homolog 1b* (*dgat1b*) were induced during infection in a Traf6-dependent manner. Furthermore, the induction of an ortholog of STEAP4 (*zgc:112143*), which has been shown to play a role in integration of inflammatory and metabolic responses, is also dependent on Traf6 (Wellen et al., 2007). We previously found this gene also to be induced by mycobacterium infection in zebrafish (Hegedus et al., 2009). The expression trend analysis shows that *pfkb3*, *hk2* and *zgc:111243* cluster together with several of the above-mentioned inflammatory genes such as *mmp9*, *mmp13*, *il1b* and *tnfb* (Fig. 5). Other metabolic functions might also play a role during infection since our analyses only show the minimal contribution of Traf6 to immunity. This is because functions that play an equally important role in immunity and development cannot confidently be analyzed in our method since we have titrated down the effect

of the morpholino treatment to have a low effect on development.

Owing to our novel approach, we have now, for the first time, been able to identify a very large group of genes whose response in infectious disease is dependent on Traf6. However, it does not come as a surprise that after knock-down of traf6 there is still an immune response to Salmonella infection, because the knock-down can be expected to be incomplete as a result of the titration of the morpholino concentration in order to avoid developmental effects. Even if it were possible to obtain viable embryos with a complete knock-down of traf6 it still would be expected that in such embryos there are innate immune responses to Salmonella infection that are independent of Traf6. For example the chemotactic response to the bacterial infection site via G-protein coupled receptors is not expected to be Traf6-dependent. Furthermore, also within the TLR-dependent pathway there are possible signaling routes that might not be dependent on Traf6. For instance, the pathway of TLR4 signaling can lead to TRAF3 activation and subsequent stimulation of the interferon pathway via the IRF3 protein. It would therefore also be interesting to use our method to analyze other key factors such as TRAF3 and partners immediately downstream of the TRAF family proteins such as TBK1 and TAB1/2/3. Such studies could show whether any of these factors might be partially redundant during the innate immune response.

## 5. Conclusions

Transcriptome profiling of traf6 knock-down allowed the identification of a gene set whose responsiveness during infection is highly dependent on Traf6. In addition, expression trend analysis identified nine clusters of genes with characteristic transcription response profiles, demonstrating that Traf6 has a dynamic role as a positive and negative regulator. We have confirmed the data from microarray experiments with whole transcriptome shotgun sequencing (RNAseq). This is one of the first times that this novel deep sequencing approach has been used for quantitative transcriptome profiling (Asmann et al., 2008; Mortazavi et al., 2008). The results show that this complementary technique gives good support for the identified Traf6-dependent infection-responsive gene set, confirming Traf6-dependent induction of 105 genes and Traf6-dependent repression of 22 genes during *S. typhimurium* infection. In addition, especially since this is the first time that RNAseq technology is used for infectious disease studies, these data represent a great wealth of disease-induced transcript information that will be of great value for future studies.

## Disclosure

The authors have no financial conflict of interest.

## Acknowledgments

We are grateful to Christiaan Henkel and Hans Jansen (ZFscreens B.V., the Netherlands) for help with RNAseq analysis and thank our group members for helpful discussions. We are also grateful to Davy de Witt, Ulrike Nehrdich and Karen Bosma for fish maintenance.

## Appendix A. Supplementary data

Supplementary data associated with this article can be found, in the online version, at doi:10.1016/j.molimm.2010.08.011.

## References

Abbott, D.W., Yang, Y., Hutti, J.E., Madhavarapu, S., Kelliher, M.A., Cantley, L.C., 2007. Coordinated regulation of Toll-like receptor and NOD2 signaling by K63-linked polyubiquitin chains. Mol. Cell. Biol. 27, 6012–6025.

Ahmad, R., Sylvester, J., Zafarullah, M., 2007. MyD88, IRAK1 and TRAF6 knockdown in human chondrocytes inhibits interleukin-1-induced matrix metalloproteinase-13 gene expression and promoter activity by impairing MAP kinase activation. Cell. Signal. 19, 2549–2557.

Asmann, Y.W., Wallace, M.B., Thompson, E.A., 2008. Transcriptome profiling using next-generation sequencing. Gastroenterology 135, 1466–1468.

Beisvag, V., Junge, F.K., Bergum, H., Jolsum, L., Lydersen, S., Gunther, C.C., Ramampiaro, H., Langaas, M., Sandvik, A.K., Laegreid, A., 2006. GeneTools – application for functional annotation and statistical hypothesis testing. BMC Bioinformatics 7, 470.

Benjamini, Y., Hochberg, Y., 1995. Controlling the false discovery rate: a practical and powerful approach to multiple testing. J. R. Stat. Soc. B 57, 289–300.

Cao, Z., Xiong, J., Takeuchi, M., Kurama, T., Goeddel, D.V., 1996. TRAF6 is a signal transducer for interleukin-1. Nature 383, 443–446.

Chakraborty, A., Brooks, H., Zhang, P., Smith, W., McReynolds, M.R., Hoying, J.B., Bick, R., Truong, L., Poindexter, B., Lan, H., Elbjeirami, W., Sheikh-Hamad, D., 2007. Stanniocalcin-1 regulates endothelial gene expression and modulates transendothelial migration of leukocytes. Am. J. Physiol. Renal Physiol. 292, F895–F904.

Chen, H.F., Jeung, E.B., Stephenson, M., Leung, P.C., 1999. Human peripheral blood mononuclear cells express gonadotropin-releasing hormone (GnRH), GnRH receptor, and interleukin-2 receptor gamma-chain messenger ribonucleic acids that are regulated by GnRH in vitro. J. Clin. Endocrinol. Metab. 84, 743–750.

Crighton, D., Wilkinson, S., O'Prey, J., Syed, N., Smith, P., Harrison, P.R., Gasco, M., Garrone, O., Crook, T., Ryan, K.M., 2006. DRAM, a p53-induced modulator of autophagy, is critical for apoptosis. Cell 126, 121–134.

Dahlquist, K.D., Salomonis, N., Vranizan, K., Lawlor, S.C., Conklin, B.R., 2002. GenMAPP, a new tool for viewing and analyzing microarray data on biological pathways. Nat. Genet. 31, 19–20.

Darnay, B.G., Ni, J., Moore, P.A., Aggarwal, B.B., 1999. Activation of NF-kappaB by RANK requires tumor necrosis factor receptor-associated factor (TRAF) 6 and NF-kappaB-inducing kinase. Identification of a novel TRAF6 interaction motif. J. Biol. Chem. 274, 7724–7731.

Davidson, A.J., Zon, L.I., 2004. The 'definitive' (and 'primitive') guide to zebrafish hematopoiesis. Oncogene 23, 7233–7246.

Davis, J.M., Clay, H., Lewis, J.L., Ghori, N., Herbomel, P., Ramakrishnan, L., 2002. Real-time visualization of mycobacterium-macrophage interactions leading to initiation of granuloma formation in zebrafish embryos. Immunity 17, 693–702.

Deng, L., Wang, C., Spencer, E., Yang, L., Braun, A., You, J., Slaughter, C., Pickart, C., Chen, Z.J., 2000. Activation of the IkappaB kinase complex by TRAF6 requires a dimeric ubiquitin-conjugating enzyme complex and a unique polyubiquitin chain. Cell 103, 351–361.

Galibert, L., Tometsko, M.E., Anderson, D.M., Cosman, D., Dougall, W.C., 1998. The involvement of multiple tumor necrosis factor receptor (TNFR)-associated factors in the signaling mechanisms of receptor activator of NF-kappaB, a member of the TNFR superfamily. J. Biol. Chem. 273, 34120–34127.

Hall, C., Flores, M.V., Crosier, K., Crosier, P., 2009. Live cell imaging of zebrafish leukocytes. Methods Mol. Biol. 546, 255–271.

Hegedus, Z., Zakrzewska, A., Agoston, V.C., Ordas, A., Racz, P., Mink, M., Spaink, H.P., Meijer, A.H., 2009. Deep sequencing of the zebrafish transcriptome response to mycobacterium infection. Mol. Immunol. 46, 2918–2930.

Herbomel, P., Thisse, B., Thisse, C., 1999. Ontogeny and behaviour of early macrophages in the zebrafish embryo. Development 126, 3735–3745.

Herbomel, P., Thisse, B., Thisse, C., 2001. Zebrafish early macrophages colonize cephalic mesenchyme and developing brain, retina, and epidermis through a M-CSF receptor-dependent invasive process. Dev. Biol. 238, 274–288.

Ishida, T., Mizushima, S., Azuma, S., Kobayashi, N., Tojo, T., Suzuki, K., Aizawa, S., Watanabe, T., Mosialos, G., Kieff, E., Yamamoto, T., Inoue, J., 1996. Identification of TRAF6, a novel tumor necrosis factor receptor-associated factor protein that mediates signaling from an amino-terminal domain of the CD40 cytoplasmic region. J. Biol. Chem. 271, 28745–28748.

Kanayama, A., Seth, R.B., Sun, L., Ea, C.K., Hong, M., Shaito, A., Chiu, Y.H., Deng, L., Chen, Z.J., 2004. TAB2 and TAB3 activate the NF-kappaB pathway through binding to polyubiquitin chains. Mol. Cell 15, 535–548.

Kawai, T., Akira, S., 2007. TLR signaling. Semin. Immunol. 19, 24–32.

Kerr, M.K., Martin, M., Churchill, G.A., 2000. Analysis of variance for gene expression microarray data. J. Comput. Biol. 7, 819–837.

Kobayashi, T., Walsh, M.C., Choi, Y., 2004. The role of TRAF6 in signal transduction and the immune response. Microbes Infect. 6, 1333–1338.

Kobayashi, T., Walsh, P.T., Walsh, M.C., Speirs, K.M., Chiffoleau, E., King, C.G., Hancock, W.W., Caamano, J.H., Hunter, C.A., Scott, P., Turka, L.A., Choi, Y., 2003. TRAF6 is a critical factor for dendritic cell maturation and development. Immunity 19, 353–363.

Koening, C.L., Miller, J.C., Nelson, J.M., Ward, D.M., Kushner, J.P., Bockenstedt, L.K., Weis, J.J., Kaplan, J., De Domenico, I., 2009. Toll-like receptors mediate induction of hepcidin in mice infected with Borrelia burgdorferi. Blood 114, 1913–1918.

Kumar, D., Nath, L., Kamal, M.A., Varshney, A., Jain, A., Singh, S., Rao, K.V., 2010. Genome-wide analysis of the host intracellular network that regulates survival of Mycobacterium tuberculosis. Cell 140, 731–743.

Lam, S.H., Chua, H.L., Gong, Z., Lam, T.J., Sin, Y.M., 2004. Development and maturation of the immune system in zebrafish, *Danio rerio*: a gene expression profiling, in situ hybridization and immunological study. Dev. Comp. Immunol. 28, 9–28.

Lesley, R., Ramakrishnan, L., 2008. Insights into early mycobacterial pathogenesis from the zebrafish. Curr. Opin. Microbiol. 11, 277–283.

Lomaga, M.A., Yeh, W.C., Sarosi, I., Duncan, G.S., Furlonger, C., Ho, A., Morony, S., Capparelli, C., Van, G., Kaufman, S., van der Heiden, A., Itie, A., Wakeham, A., Khoo, W., Sasaki, T., Cao, Z., Penninger, J.M., Paige, C.J., Lacey, D.L., Dunstan, C.R., Boyle, W.J., Goeddel, D.V., Mak, T.W., 1999. TRAF6 deficiency results in osteopetrosis and defective interleukin-1, CD40, and LPS signaling. Genes Dev. 13, 1015–1024.

Mathias, J.R., Perrin, B.J., Liu, T.X., Kanki, J., Look, A.T., Huttenlocher, A., 2006. Resolution of inflammation by retrograde chemotaxis of neutrophils in transgenic zebrafish. J. Leukoc. Biol. 80, 1281–1288.

Meeker, N.D., Trede, N.S., 2008. Immunology and zebrafish: spawning new models of human disease. Dev. Comp. Immunol. 32, 745–757.

Meijer, A.H., Gabby Krens, S.F., Medina Rodriguez, I.A., He, S., Bitter, W., Ewa Snaar-Jagalska, B., Spaink, H.P., 2004. Expression analysis of the Toll-like receptor and TIR domain adaptor families of zebrafish. Mol. Immunol. 40, 773–783.

Meijer, A.H., van der Sar, A.M., Cunha, C., Lamers, G.E., Laplante, M.A., Kikuta, H., Bitter, W., Becker, T.S., Spaink, H.P., 2008. Identification and real-time imaging of a myc-expressing neutrophil population involved in inflammation and mycobacterial granuloma formation in zebrafish. Dev. Comp. Immunol. 32, 36–49.

Min, J.Y., Park, M.H., Lee, J.K., Kim, H.J., Park, Y.K., 2009. Gonadotropin-releasing hormone modulates immune system function via the nuclear factor-kappaB pathway in murine Raw264.7 macrophages. Neuroimmunomodulation 16, 177–184.

Mogensen, T.H., 2009. Pathogen recognition and inflammatory signaling in innate immune defenses. Clin. Microbiol. Rev. 22, 240–273 (Table of Contents).

Mortazavi, A., Williams, B.A., McCue, K., Schaeffer, L., Wold, B., 2008. Mapping and quantifying mammalian transcriptomes by RNA-Seq. Nat. Methods 5, 621–628.

Munz, C., 2009. Enhancing immunity through autophagy. Annu. Rev. Immunol. 27, 423–449.

Murayama, E., Kissa, K., Zapata, A., Mordelet, E., Briolat, V., Lin, H.F., Handin, R.I., Herbomel, P., 2006. Tracing hematopoietic precursor migration to successive hematopoietic organs during zebrafish development. Immunity 25, 963–975.

Muzio, M., Natoli, G., Saccani, S., Levrero, M., Mantovani, A., 1998. The human toll signaling pathway: divergence of nuclear factor kappaB and JNK/SAPK activation upstream of tumor necrosis factor receptor-associated factor 6 (TRAF6). J. Exp. Med. 187, 2097–2101.

Naito, A., Azuma, S., Tanaka, S., Miyazaki, T., Takaki, S., Takatsu, K., Nakao, K., Nakamura, K., Katsuki, M., Yamamoto, T., Inoue, J., 1999. Severe osteopetrosis, defective interleukin-1 signalling and lymph node organogenesis in TRAF6-deficient mice. Genes Cells 4, 353–362.

O'Prey, J., Skommer, J., Wilkinson, S., Ryan, K.M., 2009. Analysis of DRAM-related proteins reveals evolutionarily conserved and divergent roles in the control of autophagy. Cell Cycle 8, 2260–2265.

Pearce, E.L., Walsh, M.C., Cejas, P.J., Harms, G.M., Shen, H., Wang, L.S., Jones, R.G., Choi, Y., 2009. Enhancing CD8 T-cell memory by modulating fatty acid metabolism. Nature 460, 103–107.

Phelps, H.A., Neely, M.N., 2005. Evolution of the zebrafish model: from development to immunity and infectious disease. Zebrafish 2, 87–103.

Redd, M.J., Kelly, G., Dunn, G., Way, M., Martin, P., 2006. Imaging macrophage chemotaxis in vivo: studies of microtubule function in zebrafish wound inflammation. Cell Motil. Cytoskeleton 63, 415–422.

Renshaw, S.A., Loynes, C.A., Trushell, D.M., Elworthy, S., Ingham, P.W., Whyte, M.K., 2006. A transgenic zebrafish model of neutrophilic inflammation. Blood 108, 3976–3978.

Solis, M., Wilkinson, P., Romieu, R., Hernandez, E., Wainberg, M.A., Hiscott, J., 2006. Gene expression profiling of the host response to HIV-1 B, C, or A/E infection in monocyte-derived dendritic cells. Virology 352, 86–99.

Sorrentino, A., Thakur, N., Grimsby, S., Marcusson, A., von Bulow, V., Schuster, N., Zhang, S., Heldin, C.H., Landstrom, M., 2008. The type I TGF-beta receptor engages TRAF6 to activate TAK1 in a receptor kinase-independent manner. Nat. Cell Biol. 10, 1199–1207.

Stein, C., Caccamo, M., Laird, G., Leptin, M., 2007. Conservation and divergence of gene families encoding components of innate immune response systems in zebrafish. Genome Biol. 8, R251.

Stockhammer, O.W., Zakrzewska, A., Hegedus, Z., Spaink, H.P., Meijer, A.H., 2009. Transcriptome profiling and functional analyses of the zebrafish embryonic innate immune response to Salmonella infection. J. Immunol. 182, 5641–5653.

Sundaram, K., Nishimura, R., Senn, J., Youssef, R.F., London, S.D., Reddy, S.V., 2007. RANK ligand signaling modulates the matrix metalloproteinase-9 gene expression during osteoclast differentiation. Exp. Cell Res. 313, 168–178.

Tanriverdi, F., Silveira, L.F., MacColl, G.S., Bouloux, P.M., 2003. The hypothalamic–pituitary–gonadal axis: immune function and autoimmunity. J. Endocrinol. 176, 293–304.

Tsukamoto, N., Kobayashi, N., Azuma, S., Yamamoto, T., Inoue, J., 1999. Two differently regulated nuclear factor kappaB activation pathways triggered by the cytoplasmic tail of CD40. Proc. Natl. Acad. Sci. U.S.A. 96, 1234–1239.

van der Sar, A.M., Musters, R.J., van Eeden, F.J., Appelmelk, B.J., Vandenbroucke-Grauls, C.M., Bitter, W., 2003. Zebrafish embryos as a model host for the real time analysis of *Salmonella typhimurium* infections. Cell. Microbiol. 5, 601–611.

Van der Sar, A.M., Stockhammer, O.W., van der Laan, C., Spaink, H.P., Bitter, W., Meijer, A.H., 2006. MyD88 innate immune function in a zebrafish embryo infection model. Infect. Immun. 74, 2436–2441.

Volkman, H.E., Pozos, T.C., Zheng, J., Davis, J.M., Rawls, J.F., Ramakrishnan, L., 2010. Tuberculous granuloma induction via interaction of a bacterial secreted protein with host epithelium. Science 327, 466–469.

Wang, C., Deng, L., Hong, M., Akkaraju, G.R., Inoue, J., Chen, Z.J., 2001. TAK1 is a ubiquitin-dependent kinase of MKK and IKK. Nature 412, 346–351.

Ward, A.C., McPhee, D.O., Condron, M.M., Varma, S., Cody, S.H., Onnebo, S.M., Paw, B.H., Zon, L.I., Lieschke, G.J., 2003. The zebrafish spi1 promoter drives myeloid-specific expression in stable transgenic fish. Blood 102, 3238–3240.

Wellen, K.E., Fucho, R., Gregor, M.F., Furuhashi, M., Morgan, C., Lindstad, T., Vaillancourt, E., Gorgun, C.Z., Saatcioglu, F., Hotamisligil, G.S., 2007. Coordinated regulation of nutrient and inflammatory responses by STAMP2 is essential for metabolic homeostasis. Cell 129, 537–548.

Willett, C.E., Cortes, A., Zuasti, A., Zapata, A.G., 1999. Early hematopoiesis and developing lymphoid organs in the zebrafish. Dev. Dyn. 214, 323–336.

Witten, P.E., Hansen, A., Hall, B.K., 2001. Features of mono- and multinucleated bone resorbing cells of the zebrafish *Danio rerio* and their contribution to skeletal development, remodeling, and growth. J. Morphol. 250, 197–207.

Wong, B.R., Josien, R., Lee, S.Y., Vologodskaia, M., Steinman, R.M., Choi, Y., 1998. The TRAF family of signal transducers mediates NF-kappaB activation by the TRANCE receptor. J. Biol. Chem. 273, 28355–28359.

Wu, H., Kerr, K., Cui, X., Churchill, G.A., 2003. MAANOVA: a software package for the analysis of spotted cDNA microarray experiments. In: Parmigiani, G., Garett, E.S., Irizarry, R.A., et al. (Eds.), The analysis of gene expression data: methods and software. Springer, Heidelberg, pp. 313–341.

Wu, S., Page, L., Sherwood, N.M., 2006. A role for GnRH in early brain regionalization and eye development in zebrafish. Mol. Cell. Endocrinol. 257–258, 47–64.

Xiao, C., Shim, J.H., Kluppel, M., Zhang, S.S., Dong, C., Flavell, R.A., Fu, X.Y., Wrana, J.L., Hogan, B.L., Ghosh, S., 2003. Ecsit is required for Bmp signaling and mesoderm formation during mouse embryogenesis. Genes Dev. 17, 2933–2949.

Yamashita, M., Fatyol, K., Jin, C., Wang, X., Liu, Z., Zhang, Y.E., 2008. TRAF6 mediates Smad-independent activation of JNK and p38 by TGF-beta. Mol. Cell 31, 918–924.

Yoshiko, Y., Maeda, N., Aubin, J.E., 2003. Stanniocalcin 1 stimulates osteoblast differentiation in rat calvaria cell cultures. Endocrinology 144, 4134–4143.